## Field Enhancement of Epsilon-near-Zero Modes in Realistic Ultra-Thin Absorbing Films

Aleksei Anopchenko<sup>1,\*</sup>, Sudip Gurung<sup>1</sup>, Subhajit Bej<sup>1</sup>, and Ho Wai Howard Lee<sup>1,2,\*</sup>

<sup>1</sup> Department of Physics, Baylor University, Waco, TX 76798, United States.

<sup>2</sup> The Institute for Quantum Science and Engineering, Texas A&M University, College Station, TX 77843, United States.

Using basic considerations on the average power absorbed in ultra-thin conducting films, we derive a closed-form expression for the average electric-field intensity enhancement (FIE) due to epsilon-near-zero (ENZ) polariton modes. We show that FIE in ENZ media with realistic losses reaches a maximum value in the limit of ultra-small film thickness. The maximum value is reciprocal to the second power of ENZ losses. This is illustrated in an exemplary series of aluminum-doped zinc oxide nanolayers of varying thickness grown by atomic layer deposition technique. The limiting behavior of FIE is shown in exact cases of the perfect absorption, normal incidence, and in a case of ultra-thin lossless ENZ films. Only in the case of lossless ENZ films FIE is inversely proportional to the second power of film thickness as it was predicted by S. Campione, et al. [Phys. Rev. B 91, 121408(R) (2015)]. We also show that FIE could achieve values as high as 100,000 in ultra-thin polar semiconductor films, which have losses as small as 0.02 close to the longitudinal optic (LO) phonon frequency.

Electromagnetic filed confinement and field intensity enhancement (FIE) of metal nanostructures are fundamental components of plasmonics and nanophotonics and the base of plasmonic and metamaterials technologies [1-3]. Intrinsic loss and nonlocality of the dielectric response of metal nanostructures limit FIE [3,4] and so present a significant challenge to plasmonic technologies [5,6]. Recently, conductive materials with vanishing real part of electric permittivity, i.e.  $Re(\varepsilon) \to 0$ , or epsilon-near-zero (ENZ) materials are found to be beneficial for strong field confinement in subwavelength dimensions. ENZ media with very low (zero) intrinsic loss, i.e.  $Im(\varepsilon) \to 0$ , have near-zero refractive index and very unusual wave dynamics [7-9]. Loss of ENZ media affects their optical properties, e.g. induce the anti-Snell's law of refraction [10,11], but also limits the performance of ENZ materials [12-14]. Several solutions to the loss reduction have been proposed, e.g. using gain-media [12] and structural dispersion engineering [15]. Ultra-thin films of ENZ media under TM-polarized excitation support plasmon-polariton modes near the ENZ frequency, the so-called ENZ modes [16-18]. The excitation of these ENZ modes leads to an enhanced optical local density of states and therefore to an enhanced absorption and FIE. Some aspects of the polariton resonances in ENZ slabs with negligible-to-moderate losses, i.e.  $Im(\varepsilon) \ll 1$ , have been discussed in Ref. [19]. For example, it has been shown that the quality factor of polariton resonance in term of angular bandwidth is weakly affected by the presence of the moderate losses. A model describing transmission, reflection, and absorption coefficients and local FIE in subwavelength ENZ slabs have been presented in Ref. [20]. However, the analysis mainly deals with lossless and loss-compensated ENZ metamaterials and only briefly discuss the effects of losses [21]. FIE dependence on the thickness of ultra-thin ENZ films has been shown in Ref. [18], but limited to the lossless case. Large and almost independent of the film thickness FIE is shown in Ref [22] in a uniaxially anisotropic ENZ film with both transverse and longitudinal loss of  $Im(\varepsilon) = 0.001$ -0.05, an alternative metamaterial to lossy isotropic EZN films.

In this letter, using basic considerations on power absorbed in isotropic ultra-thin ENZ films, we derive a closed-form expression for an average FIE in realistic ENZ media with inherent optical loss. Quantitative description of the FIE dependence on the intrinsic losses of ENZ films was still missing. We show the dependence of FIE on absorptance of ultra-thin ENZ film due to the excitation of polariton modes and discuss FIE asymptotic values in the limits of ultra-small ENZ film thickness and loss. Absorptance of ENZ films is obtainable experimentally and thus FIE could be readily maximized for emerging applications of ENZ media. The limiting behavior of FIE is shown in the following three cases:

- 1. The perfect absorption due to ENZ mode excitation;
- 2. Normal incidence of light and finite ENZ losses;
- 3. Oblique incidence and infinitesimal losses.

We consider an ultra-thin absorbing film of permittivity  $\varepsilon(\lambda) = \text{Re}(\varepsilon) + i \text{ Im}(\varepsilon)$  and thickness, d, bounded by two semi-infinite media: incident medium with refractive index  $n_0$  and the substrate with refractive index  $n_s$  (generally complex) (Fig. 1). The film is illuminated by TM-polarized plane wave at an angle of incidence  $\theta_0$ . The film thickness normalized to the wavelength of incident light,  $\lambda$ , and permittivity satisfy the following conditions:

$$\delta = \frac{2\pi d}{\lambda} \ll 1 \text{ and } \operatorname{Re}(\varepsilon) \to 0 \land \left| \operatorname{Re}(\varepsilon) \right| << \operatorname{Im}(\varepsilon). \tag{1}$$

The last inequality with vanishing real part of permittivity defines ENZ medium, but also reflects the fact that realistic ENZ media could have high material loss. For example, aluminum-doped zinc oxide (ZnO:Al) has permittivity described by the Drude model in a wavelength range adjacent to ENZ wavelength with  $Im(\varepsilon) \sim 1$  at ENZ wavelength [23].

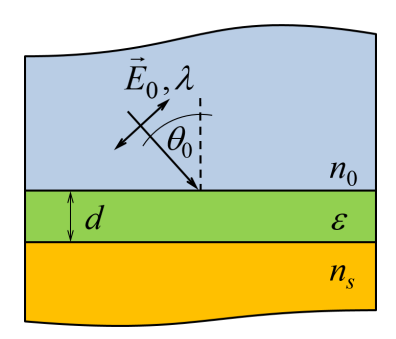


Fig. 1. Schematic of the ultra-thin ENZ film of thickness d and permittivity  $\varepsilon$  illuminated by TM-polarized light of wavelength  $\lambda$  at an angle of incidence  $\theta_0$ . The incidence medium and substrate have refractive index  $n_0$  and  $n_s$ , respectively;  $n_0$  is real, while  $n_s$  could be complex (e.g., metal).

The considered ultra-thin absorbing ENZ film supports plasmon-polariton modes described by the following dispersion relationship [16,18]:

$$(\varepsilon_s \eta_0 + \varepsilon_0 \eta_s) \varepsilon = i\delta (\varepsilon^2 \eta_0 \eta_s + \varepsilon_0 \varepsilon_s \xi), \qquad (2)$$

where  $\varepsilon_j = n_j^2$ ,  $\eta_j = \sqrt{\varepsilon_j - n_e^2}$  (j = 0, s),  $\xi = \varepsilon - n_e^2$ , and  $n_e = n_0 \sin(\theta_0)$ . The solutions of Eq. (2) are sought by assuming complex-valued  $\lambda$  and real-valued  $n_e$  [24]. Depending on a value of the ratio of the refractive indexes of surrounding media, or refractive index contrast  $v = n_s/n_0$ , there are three different solutions of Eq. (2) or Modes 1-3:

- a) Mode 1 a bound ENZ mode if both  $n_0$  and  $n_s$  are real and v < 1 [16,18].
- b) Mode 2 a radiative ENZ mode if both  $n_0$  and  $n_s$  are real and v > 1 [25].
- c) Mode 3 a radiative Berreman mode if  $n_s$  is complex, e.g. the substrate is metal [17,26].

Figure 2 shows an example of the dispersion characteristics Eq. (2) for the Mode 1-3 in a ZnO:Al nanolayer with a thickness of 58 nm grown by atomic layer deposition (ALD) (for details on fabrication and optical properties of ZnO:Al nanolayers see [23]). The permittivity of the nanolayer is described by the Drude model:  $\varepsilon = \varepsilon_{\infty} - \omega_p^2 / (\omega^2 + i\omega\Gamma)$ , where  $\varepsilon_{\infty} = 3.7$ , plasma frequency  $\omega_p = 2.4 \times 10^{15}$  Hz, and electron collision rate  $\Gamma = 2.8 \times 10^{14}$  Hz. The dispersion characteristics are close to the ENZ wavelength,  $\lambda_{\rm ENZ}$ . In this letter, we will study the dependence of an average FIE on optical losses and the thickness of ultra-thin ENZ films that support these three ENZ modes.

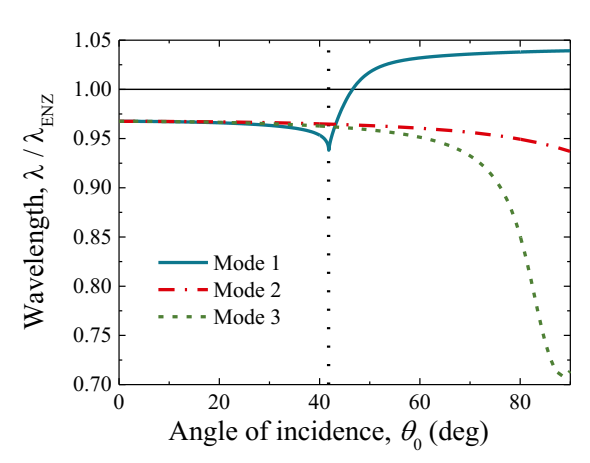


Fig. 2. An example of the dispersion characteristics for the Mode 1-3 supported by a ZnO:Al nanolayer with a thickness of 58 nm [23]. The ENZ wavelength,  $\lambda_{\rm ENZ}$ , is 1562 nm. The vertical dotted line shows the critical angle of 41.8° for the Mode 1. In the calculation we assume that the permittivity of the ZnO:Al nanolayer is described by the Drude model. We also assume  $n_0 = 1.5$  and  $n_s = 1$  for Mode 1,  $n_0 = 1$  and  $n_s = 1.44$  for Mode 2, and  $n_0 = 1$  and  $n_s = 0.34 + i11$  (gold) for Mode 3.

Excitation of the ENZ modes leads to enhanced photonic local density of states (LDOS) and hence enhanced absorptance and FIE in ultra-thin ENZ films. The absorbed power per unit

volume of an isotropic conducting film in harmonic electromagnetic fields with the time dependence of  $e^{-i\omega t}$  can be calculated from the divergence of the Poynting vector  $\vec{S} = \vec{E} \times \vec{H}$  [27]:

$$P_{vol} = \left\langle -div(\vec{S}) \right\rangle = \left\langle \vec{E} \cdot curl \vec{H} - \vec{H} \cdot curl \vec{E} \right\rangle = \left\langle \vec{E} \cdot \frac{\partial \vec{D}}{\partial t} + \vec{H} \cdot \frac{\partial \vec{B}}{\partial t} \right\rangle =$$

$$= \frac{1}{2} \operatorname{Re} \left( i\omega \vec{E} \cdot \overrightarrow{D}^* + i\omega \vec{H} \cdot \overrightarrow{B}^* \right) = \frac{1}{2} \omega \left( \varepsilon_0 \operatorname{Im}(\varepsilon) \left| \vec{E} \right|^2 + \mu_0 \operatorname{Im}(\mu) \left| \vec{H} \right|^2 \right), \tag{3}$$

where the angle brackets mean time average. Another derivation of the last equation in Eq. (3) is shown in [28]. Using Eq. (3), we derive the following expression for an average absorbed power per unit area of non-magnetic films:

$$P = \frac{1}{2}\omega\varepsilon_0 \operatorname{Im}(\varepsilon) |E|^2 \frac{d}{\cos(\theta_0)}.$$
 (4)

Here, *E* is the average (integrated over the film thickness) electric field inside the film, which is different from a local field that depends on spatial coordinates. The power of the incident plane wave per unit area and unit time is:

$$P_0 = \frac{1}{2} c n_0 \varepsilon_0 \left| E_0 \right|^2, \tag{5}$$

where  $E_0$  is the incident field,  $n_0$  is the refractive index of the incidence medium. From Eqs. (4) and (5), we find that absorptance is:

$$A = \frac{P}{P_0} = \frac{\omega d \operatorname{Im}(\varepsilon)}{c n_0 \cos(\theta_0)} \left| \frac{E}{E_0} \right|^2 = \delta \frac{\operatorname{Im}(\varepsilon)}{n_0 \cos(\theta_0)} \left| \frac{E}{E_0} \right|^2. \tag{6}$$

Therefore, FIE can be calculated from the absorptance using Eq. (6):

$$FIE = \left| \frac{E}{E_0} \right|^2 = \frac{n_0 A(\delta, \varepsilon, \theta_0) \cos(\theta_0)}{\delta \operatorname{Im}(\varepsilon)}. \tag{7}$$

It is noteworthy that Eq. (7) has general validity, i.e. it is valid regardless of the excitation of a particular ENZ mode. It is also the average FIE inside the ENZ film that is different from a local FIE at the plane wave impinging boundary of the film discussed in [20]. The optical losses and thickness of the ENZ material enters in (7) directly as  $Im(\varepsilon)$  and  $\delta$  and indirectly through the absorptance A. In order to show the total effect of the losses and thickness on FIE we have to complement Eq. (7) with the expression for absorptance of ultra-thin ENZ film. Reflection and transmission of plane waves incident upon an ENZ medium has been studied in [20,29,30]. Complex reflection and transmission coefficients of an ENZ slab for certain limiting conditions has been analyzed in [19,20]. We use another approach based upon the work by Abeles [31]. The absorptance of ultra-thin ENZ film illuminated by TM-polarized plane wave under oblique incidence [31,32]:

$$A = 1 - R - T$$
,  $R = |r|^2$ , and  $T = (\text{Re}(Z_s)/Z_0) \cdot |t|^2$ , (8)

where R and T are the reflectance and transmittance, respectively, and  $Z_j = n_j / \cos(\theta_j)$  is the wave admittance of the j-medium (j = 0, s). The complex reflection and transmission coefficients, r and t, respectively, are given by:

$$r = \frac{\left(m_{11} + m_{12} \cdot Z_s\right) Z_0 - \left(m_{21} + m_{22} \cdot Z_s\right)}{\left(m_{11} + m_{12} \cdot Z_s\right) Z_0 + \left(m_{21} + m_{22} \cdot Z_s\right)},\tag{9}$$

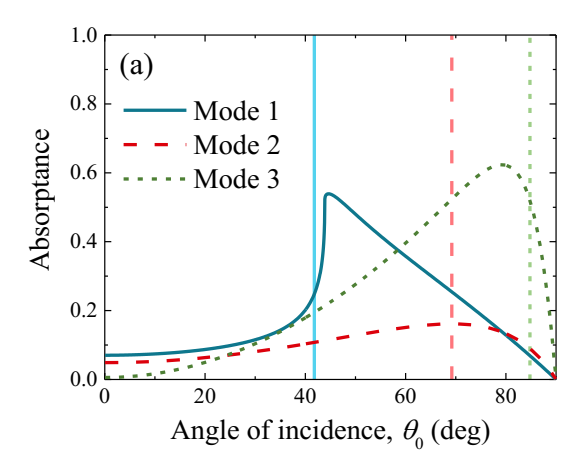
$$t = \frac{2Z_0}{(m_{11} + m_{12} \cdot Z_s)Z_0 + (m_{21} + m_{22} \cdot Z_s)}. (10)$$

Here  $m_{kl}$  (k, l = 1, 2) are the elements of the characteristic matrix:

$$[M] = \begin{bmatrix} 1 - \xi \frac{\delta^2}{2} & -i \frac{\xi}{\varepsilon} \delta \\ -i\varepsilon \delta & 1 - \xi \frac{\delta^2}{2} \end{bmatrix}. \tag{11}$$

The reflectance and transmittance in Eq. (8) are calculated at the top and bottom interfaces of ENZ film, respectively (see Fig. 1). It is noteworthy that the dispersion relationship (Eq. (2)) could be obtained by finding poles of the complex reflection coefficient r, Eq. (9).

Using Eqs. (7) and (8) we can calculate the absorptance and FIE in ENZ media. An example of such calculations is given below for a ZnO:Al nanolayer at the ENZ wavelength of 1627 nm for the three ENZ modes (Fig. 3). The nanolayer has a thickness of 22 nm and is grown by ALD (for details on fabrication and characterization of ZnO:Al nanolayers see [23]). The absorptance and FIE curves show the maxima due to the excitation of the ENZ modes.



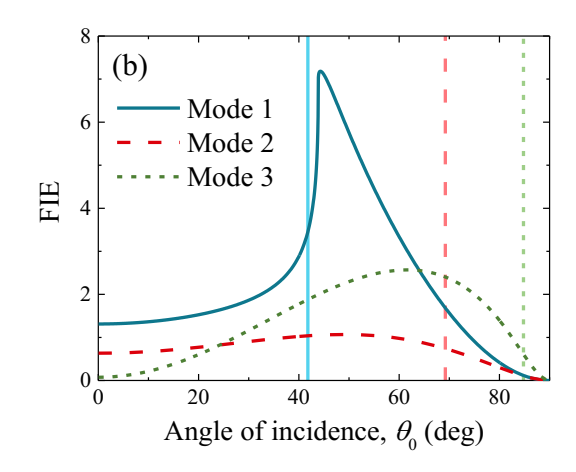


Fig. 3. Angular dependence of (a) absorptance and (b) FIE for a ZnO:Al nanolayer with a thickness of 22 nm at the ENZ wavelength of 1627 nm ( $\delta$ = 0.08, Im( $\varepsilon$ ) = 0.9) for the three ENZ modes: Mode 1 – a bound mode with  $n_0$  = 1.5 and  $n_s$  = 1, Mode 2 – a radiative mode with  $n_0$  = 1 and  $n_s$  = 1.44, and Mode 3 – a radiative mode with  $n_0$  = 1 and  $n_s$  = 0.34 + i 11 (gold). The vertical lines are: the critical angle of 41.8°, the quasi-Brewster angle of 69.2° (Eq. (12)), and the pseudo-Brewster angle of 84.8°.

The angular position of the absorptance maxima is determined by the coupling conditions to a particular mode at a wavelength of interest (see Eq. (2)), e.g. the ENZ wavelength in this example. The dependence of the absorptance maxima on the thickness and loss of an ENZ film for the three modes is presented in the Supplemental Material. For ultra-thin ENZ films,

 $\delta \ll \text{Im}(\varepsilon)$ , the absorptance maximum for Mode 1 is found at the critical angle,  $\theta_c = \arcsin(v)$ . The angle of the absorptance maximum for Mode 2 is given by the following expression:

$$\theta_{q-B} = \arccos\left[\frac{(v^2 - 1)\sqrt{v^2 + 1}}{v^4 + 1}\right].$$
 (12)

We will be calling this angle a quasi-Brewster angle because it differs from the Brewster angle,  $\theta_B = \arctan(\nu)$ , especially when  $\nu \approx 1$  (Fig. 4). The Eq. (12) is obtained by finding the pole of the complex reflection coefficient (Eq. (9)) at a limit of zero ENZ film thickness. The angle of the absorptance maximum for Mode 3 is the pseudo-Brewster angle. The real-value solution of the pseudo-Brewster angle for the case of absorbing (complex-value) substrates is given in [33]. The angle of the absorptance maximum for all three modes is a function of the refractive index contrast  $\nu$ . This dependence for the real-value refractive index contrast is shown in Fig. 4. The FIE maxima (Fig. 3b) that correspond to the absorptance maxima in Fig. 3a are shifted to smaller angles because of the  $\cos(\theta_0)$  term in the Eq. (7).

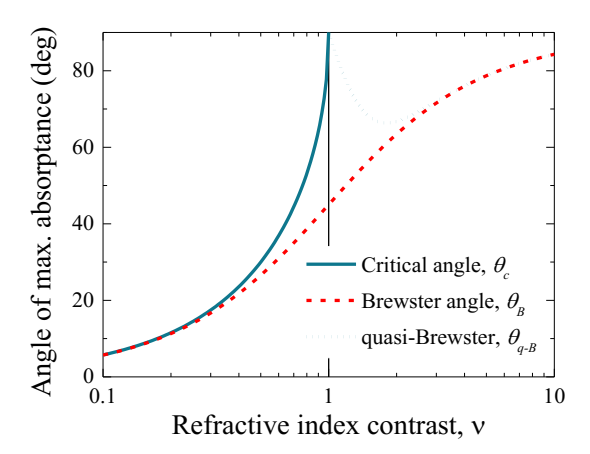
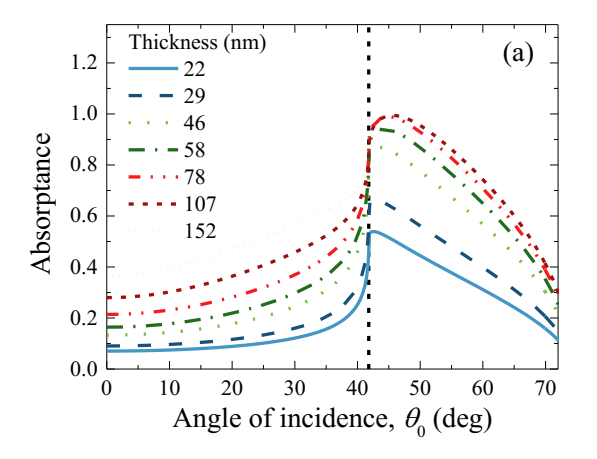


Fig. 4. The angle of the absorptance maximum as a function of the real-valued refractive index contrast  $\nu$ . The angle is the critical angle for Mode 1 ( $\nu$ < 1) and the quasi-Brewster angle of Eq. (12) for Mode 2 ( $\nu$ > 1).

We first consider the Mode 1 in a series of ZnO:Al nanolayers with varying thickness. In a case of absorbing ENZ films, the absorptance maxima are approaching the critical angle of 41.8° when the film thickness decreases (Fig. 5). Absorptance of an ultra-thin ENZ film at the critical angle is proportional to the film thickness

$$A(\theta \to \theta_c) \approx \frac{4\delta}{\delta_{th}} \tag{13}$$

if the film thickness satisfies the following condition:



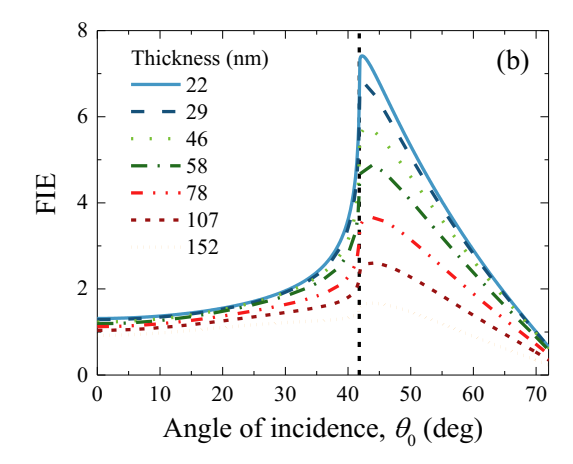


Fig. 5. Angular dependence of (a) absorptance and (b) FIE for a series of ZnO:Al nanolayers with varying thickness (see the legend) for the Mode 1 at the ENZ wavelength (cf. Fig. 3). The vertical dashed line shows the critical angle of 41.8°.

$$\delta \ll \delta_{th} = \frac{\sqrt{n_0^2 - n_s^2}}{n_0^2 n_s^2} \operatorname{Im}(\varepsilon). \tag{14}$$

It can be shown that the linear relationship (14) between thickness and loss is the same with the one obtained in [34,35] for the perfect absorption in ultra-thin ENZ films. Substituting Eq. (13) into Eq. (7), we find an asymptotic value of FIE achievable in ultra-thin absorbing ENZ films due to the Mode 1:

$$FIE(\theta \to \theta_c) = \frac{4n_0^2 n_s^2}{\text{Im}(\varepsilon)^2}.$$
 (15)

It is important that FIE is reciprocal of the second power of the ENZ material losses. In our example of ZnO:Al nanolayers [23], the condition (14) is satisfied for the nanolayer thicknesses much smaller than 107 nm (the value of  $\delta_{th} \approx 0.45$ ) and a value of the maximum FIE calculated from Eq. (7) for the thinnest nanolayer is 8 (Fig. 6). This value approaches the asymptotic value of 11 for the average FIE in the ZnO:Al nanolayers calculated using Eq. (15). It is important that the FIE for Mode 1 could achieve values as high as 100,000 in ultra-thin polar semiconductor films, such as aluminum nitride (AlN), which have losses as small as 0.02 close to the longitudinal optic (LO) phonon frequency of 27 THz. This follows from the Eq. (15). FIE values larger than 3,600 has been shown for AlN polaritons in [36] but for Mode 3, which we discuss later.

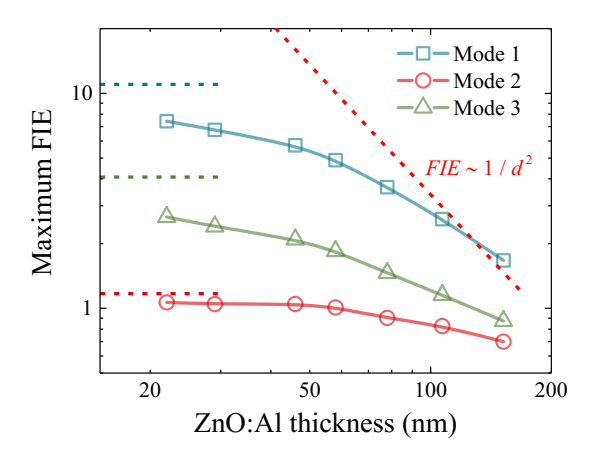


Fig. 6. Thickness dependence of the maximum FIE for a series of ZnO:Al nanolayers with varying thickness for the three ENZ modes at the ENZ wavelength: Mode 1 - a bound mode excited in the Kretschmann configuration ( $n_0 = 1.5$ ,  $n_s = 1$ ), Mode 2 - a radiative mode in the nanolayer supported by glass ( $n_0 = 1$ ,  $n_s = 1.44$ ), and Mode 3 - a radiative mode in the nanolayer supported by metal (gold) ( $n_0 = 1$ ,  $n_s = 0.34 + i$  11). Red dash curve shows  $1/d^2$  dependence in the limit of zero losses. Horizontal dashed lines show the asymptotic values of the maximum FIE, namely 1.2, 4.1, and 11.0 for Mode 2, Mode 3, and Mode 1, respectively.

As the thickness of the ENZ film increases the absorptance increases and at a certain thickness reaches unity or the perfect absorption (Fig. 5a). In the case of the perfect absorption, i.e. A = 1, the thickness of the ENZ film normalized to the perfect absorption wavelength,  $\delta$ , satisfies the critical coupling condition [34,35,37,38] and is related to the permittivity of the ENZ film and the angle of incidence as follows:

$$\frac{1}{\delta} = \frac{n_0^3 \operatorname{Im}(\varepsilon) \sin(\theta_0) \tan(\theta_0)}{\operatorname{Re}(\varepsilon)^2 + \operatorname{Im}(\varepsilon)^2}.$$
 (16)

Substituting (16) into (7) gives FIE at the perfect absorption condition:

$$FIE = \frac{n_0^4 \sin^2(\theta_0)}{\text{Re}(\varepsilon)^2 + \text{Im}(\varepsilon)^2}.$$
 (17)

Therefore, at the perfect absorption conditions, FIE is inversely proportional to the second power of ENZ losses (if the perfect absorption wavelength is equal to ENZ wavelength then  $Re(\varepsilon) = 0$ ). It should be noted that FIE of the perfect absorption Eq. (17) is thickness dependent because of the thickness dependence of the perfect absorption angle and ENZ mode dispersion. For the Mode 1 considered above, the perfect absorption occurs at the critical angle (Fig. 5), i.e. at the same angle as the maximum asymptotic FIE value of ultra-thin ENZ films (cf. Eq. (15)). FIE in thicker ENZ films with the perfect absorption (Eq. (17)) is smaller than the maximum FIE value of ultra-thin ENZ films (Eq. (15)) by an approximate factor of 4 (Fig. 6).

In the case of Mode 2 and Mode 3, the maximum absorptance occurs at the quasi- and pseudo-Brewster angles, respectively (Fig. 3a), and is proportional to the ENZ film thickness to the first-order in  $\delta$  ( $\delta$ << Im( $\varepsilon$ )). Therefore, FIE is thickness independent (cf. Eq. (7)) and limited in lossy ultra-thin ENZ films (Fig. 7). The limiting FIE values of Mode 2 and Mode 3 are smaller than the FIE value of Mode 1, Eq. (15) (Fig. 6). Also, similar to Mode 1, FIE is inversely proportional to the second power of ENZ losses for Mode 2 and Mode 3 (Fig. 7).

Maximizing FIE needs minimizing ENZ losses. In order to illustrate the effect of losses on the FIE in ultra-thin ENZ layers, we calculated the angular and thickness dependences of the FIE maximum for a range of loss values found in realistic ENZ media and the results are shown in Fig. 7. It is seen from the figure that FIE reaches its maximum value for the thickness  $\delta << \text{Im}(\varepsilon)$ . The FIE increases with decreasing losses as  $1/\text{Im}(\varepsilon)^2$ . For a fixed ENZ losses, FIE of Mode 1 decreases as the film thickness increases and, after reaching a certain thickness threshold, decreases at a slower pace at angles much smaller than the critical angle. For larger film thickness, the FIE dependence for Mode 1 resembles the one for Mode 2 (see black dotted lines in Fig. 7a).

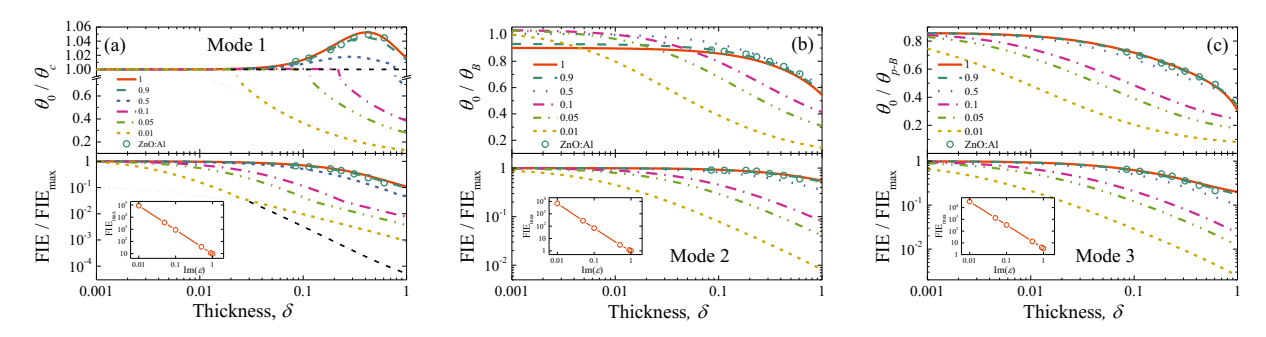


Fig. 7. Thickness and angular dependence of normalized FIE values for Mode 1 (a), Mode 2 (b), and Mode 3 (c) at ENZ wavelength. The refractive indexes are the same as in Fig. 2 and Fig. 3 and loss values are shown in the legend. Open green circles shows experimental ZnO:Al data. Insets show the  $1/\text{Im}(\varepsilon)^2$  dependence of the maximum FIE (at  $\delta \le 0.001$ ). The maximum FIE is used to normalize FIE data. The critical, Brewster, and pseudo-Brewster angles are used to normalize FIE angles for Mode 1, Mode 2, and Mode 3, respectively. The black dash-dot line in (a) shows FIE at the critical angle and black dot lines show FIE and angle of the corresponding Mode 2 (FIE is normalized to the maximum FIE of Mode 1).

Figure 8 shows calculated angular dependences of absorptance and FIE in an ZnO:Al nanolayer with a fixed thickness of 22 nm and varying ENZ losses at the ENZ wavelength. As losses become smaller than the film thickness, i.e.  $\text{Im}(\varepsilon) < \delta$ , the maximum absorptance and FIE occur below the critical angle (cf. Fig. 7). This result is in an agreement with the one in [20].

We consider now the limiting case of infinitesimal ENZ losses (although realistic ENZ materials always have some loss), the absorptance become zero and FIE approaches the following limit:

$$FIE \to \frac{4\left(\cot\left(\theta_0\right)\right)^2}{n_0^2 \delta^2} \,. \tag{18}$$

Equation (18) shows that, first, FIE in an ENZ film of a certain thickness become large and increases towards the small angles of incidence as the losses become infinitesimal (Fig. 8b). Second, FIE at a fixed angle is very large and scales with the thickness of ENZ film as the power-law with an exponent of -2 (see Eq. (18)). The later result agrees with the result in [18,20,22]. However, in realistic absorbing ENZ films with  $Im(\varepsilon) \neq 0$ , the FIE increases weaker then  $1/\delta^2$ . In our ZnO:Al nanolayers with the losses  $Im(\varepsilon) \sim 1$  at the ENZ wavelength, FIE reaches the value of 8 in the thinnest nanolayer (Fig. 6).

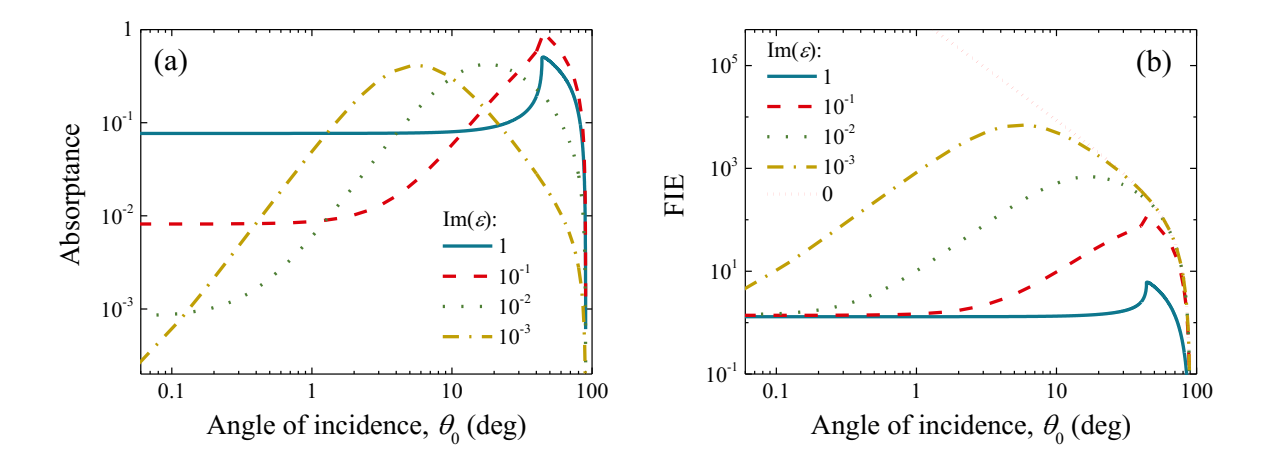


Fig. 8. Angular dependence of (a) absorptance and (b) FIE of Mode 1 in ultra-thin ENZ film with a fixed thickness of 22 nm and varying ENZ losses (see the legend) at the ENZ wavelength of 1627 nm ( $\delta$ = 0.08). In the calculations we use  $n_0$  = 1.5 and  $n_s$  = 1. The red dotted line in (b) shows the limiting case of infinitesimal ENZ losses Eq. (18).

In the case of very small but finite material losses and the normal incidence, i.e.  $\theta = 0^{\circ}$ , absorptance to the first-order approximation in  $\delta$  is:

$$A(\theta = 0^{\circ}) \approx \delta \frac{4n_0 \operatorname{Im}(\varepsilon)}{(n_0 + n_s)^2}.$$
 (19)

From (19) it follows:

$$FIE(\theta = 0^{\circ}) = \frac{4n_0^2}{(n_0 + n_s)^2}.$$
 (20)

Therefore, FIE at normal incidence is small (Fig. 8) and does not depend on the material losses (which, however, are finite), ENZ mode ( $n_s$  is real), and ENZ layer thickness if  $\delta << 1$ .

In conclusions, we derive a closed-form analytical expression for the average electric-field intensity enhancement due to the radiative and bound ENZ modes in ultra-thin layers with non-negligible optical losses – the real-world ENZ media. We show the dependence of FIE on losses of ENZ films and the film thickness. In absorbing ENZ films, FIE reaches a limiting value at the limit of deep subwavelength thicknesses. The limiting FIE value is reciprocal to the second power of the ENZ losses. In the case of lossless films, FIE can be described by a power-law dependence on film thickness with the exponent of -2 predicted by S. Campione, et al. [18]. We illustrate our analysis of the FIE dependence on ENZ film thickness with an example of ZnO:Al nanolayers of varying thicknesses grown by ALD. This study is important for maximizing FIE in nonlinear ENZ media [39] and applications of ENZ media in quantum plasmonics [40,41].

This work was supported in part by the AFOSR-AOARD (Award number: FA2386-18-1-4099), Defense Advanced Research Projects Agency (grant number N66001-17-1-4047), CAREER Award Program from National Science Foundation (grant number: 1752295), Robert A. Welch Foundation (Award number: AA-1956-20180324).

## References

- A. M. Urbas et al., Journal of Optics 18, 53, 093005 (2016).
- [2] I. S. Mark et al., Journal of Optics 20, 043001 (2018).
- R. Gordon and A. Ahmed, ACS Photonics 5, 4222 (2018). [3]
- [4] C. Ciraci, R. T. Hill, J. J. Mock, Y. Urzhumov, A. I. Fernandez-Dominguez, S. A. Maier, J. B. Pendry, A. Chilkoti, and D. R. Smith, Science 337, 1072 (2012).
- J. B. Khurgin, Nature Nanotechnology 10, 2 (2015). [5]
- S. V. Boriskina et al., Advances in Optics and Photonics 9, 775 (2017). [6]
- [7] I. Liberal and N. Engheta, Nature Photonics 11, 149 (2017).
- X. X. Niu, X. Y. Hu, S. S. Chu, and Q. H. Gong, Advanced Optical Materials 6, 36, 1701292 (2018). [8]
- [9] N. Kinsey, C. DeVault, A. Boltasseva, and V. M. Shalaev, Nature Reviews Materials 4, 742 (2019).
- S. Feng, Physical Review Letters 108, 193904 (2012). [10]
- [11] L. Sun, S. Feng, and X. Yang, Applied Physics Letters 101, 241101 (2012).
- D. de Ceglia, S. Campione, M. A. Vincenti, F. Capolino, and M. Scalora, Physical Review B 87, 155140 (2013). [12]
- M. H. Javani and M. I. Stockman, Physical Review Letters 117, 107404 (2016). [13]
- Γ141 D. Rocco, C. De Angelis, D. de Ceglia, L. Carletti, M. Scalora, and M. A. Vincenti, Optics Communications 456, 124570 (2020).
- Y. Li, I. Liberal, and N. Engheta, Science Advances 5, eaav3764 (2019). [15]
- F. Z. Yang, J. R. Sambles, and G. W. Bradberry, Physical Review B 44, 5855 (1991). [16]
- S. Vassant, J.-P. Hugonin, F. Marquier, and J.-J. Greffet, Optics Express 20, 23971 (2012). [17]
- Γ181 S. Campione, I. Brener, and F. Marquier, Physical Review B 91, 121408, 121408 (2015).
- A. Alu, M. G. Silveirinha, A. Salandrino, and N. Engheta, Physical Review B 75, 155410, 155410 (2007). [19]
- [20] S. Campione, D. de Ceglia, M. A. Vincenti, M. Scalora, and F. Capolino, Physical Review B 87, 035120, 035120 (2013).
- D. de Ceglia, S. Campione, M. A. Vincenti, F. Capolino, and M. Scalora, Physical Review B 87, 12 (2013). [21]
- [22] M. Kamandi, C. Guclu, T. S. Luk, G. T. Wang, and F. Capolino, Physical Review B 95, 161105, 161105 (2017).
- [23] S. Gurung, A. Anopchenko, S. Bej, J. Joyner, J. D. Myers, J. Frantz, and H. W. Lee.
- [24] A. Archambault, T. V. Teperik, F. Marquier, and J. J. Greffet, Physical Review B 79, 8, 195414 (2009).
- [25] S. Campione, I. Kim, D. de Ceglia, G. A. Keeler, and T. S. Luk, Optics Express 24, 18782 (2016).
- [26] D. W. Berreman, Physical Review 130, 2193 (1963).
- L. D. Landau, E. M. Lifshits, and L. P. Pitaevskiĭ, Electrodynamics of continuous media (Pergamon, Oxford Oxfordshire; New York, [27] 1984), 2nd edn., Course of theoretical physics / L D Landau & E M Lifshitz, 8.
- J. M. Hao, L. Zhou, and M. Qiu, Physical Review B 83, 165107, 165107 (2011). [28]
- [29] S. Feng, Physical Review Letters 108, 193904, 193904 (2012).
- Z. Xu and H. F. Arnoldus, OSA Continuum 2, 722 (2019). [30]
- [31] F. Abeles, Journal of the Optical Society of America 47, 473 (1957).
- W. N. Hansen, Journal of the Optical Society of America 58, 380 (1968). [32]
- [33] S. Y. Kim and K. Vedam, Journal of the Optical Society of America A-Optics Image Science and Vision 3, 1772 (1986).
- S. Feng and K. Halterman, Physical Review B 86, 165103, 165103 (2012). [34]
- [35] T. S. Luk et al., Physical Review B 90, 085411, 085411 (2014).
- [36] N. C. Passler, I. Razdolski, D. S. Katzer, D. F. Storm, J. D. Caldwell, M. Wolf, and A. Paarmann, ACS Photonics 6, 1365 (2019).
- [37] M. A. Badsha, Y. C. Jun, and C. K. Hwangbo, Optics Communications 332, 206 (2014).
- A. Anopchenko, L. Tao, C. Arndt, and H. W. H. Lee, ACS Photonics 5, 2631 (2018). [38]
- [39] O. Reshef, I. De Leon, M. Z. Alam, and R. W. Boyd, Nature Reviews Materials 4, 535 (2019).
- [40] M. S. Tame, K. R. McEnery, S. K. Ozdemir, J. Lee, S. A. Maier, and M. S. Kim, Nature Physics 9, 329 (2013).
- [41] A. Sivan and M. Orenstein, Physical Review B 99, 115436, 115436 (2019).

\* Corresponding authors: Oleksiy Anopchenko@baylor.edu; Howard Lee@baylor.edu